

RESEARCH ARTICLE

Electro-polymerization of poly Eugenol on Ti and Ti alloy dental implant treatment by micro arc oxidation using as Anti-corrosion and Anti-microbial

Haider Abdulkareem AlMashhadani¹, Khulood Abed Saleh²

¹AlRasheed University College, Dentistry Department

²Department of Chem., College of Science, Baghdad University, Jaderyah, Baghdad, Iraq

*Corresponding Author E-mail: H_R200690@yahoo.com

ABSTRACT:

In this work, electrochemical process was presented to polymerized eugenol on Gr.2 and Gr.5 titanium alloys before and after treated by Micro Arc Oxidation (MAO), where Gr.2 is commercial pure titanium and Gr.5 is Ti-6Al-4V dental alloys. The deposited layers were characterized by scanning electron microscopy (SEM), energy-dispersive X-ray spectroscopy (EDS), X-ray diffraction (XRD), and Fourier transform infrared spectroscopy (FTIR). The adhesion strength of polymeric thin-film was estimation by using pull-off adhesion test and the result was the adhesion strength of PE was (1.23 MPa) on Gr.2 before MAO and increase to (1.98 MPa) on Gr.2 after MAO treatment. The corrosion behavior of Gr.2 and Gr.5 alloy in artificial saliva environment at temperature ranged 293-323K has been studied and assessed by means of electrochemical technique potentiodynamic polarization curves. The corrosion protection increased to 63% and 80% after coated blank Gr.2 and Gr.5 by PE, while when deposition PE on treated Gr.2 and Gr.5 by MAO, the protection efficiency (I%) increase to 68% and 81% respectively at 323K. The antimicrobial activities of the samples were evaluated against different bacteria and oral fungi (Candia), PE coating show antibacterial activity (28 and 25 mm) against S.aureus and B.Subtilis respectively and show antifungal activity (29 and 24 mm) against C.albicans and C.glabrata oral fungi respectively.

KEYWORDS: PolyEugenol, Eugenol, Titanium alloy, MAO.

1. INTRODUCTION:

Micro arc oxidation (MAO) is one of the most promising techniques for metal and alloy surface therapy and has subsequently been widely accepted by multiple industries branches. MAO is usually used on valve materials such as Al, Mg, Ti, Ta, Nb, Zr, and Be to create multi-purpose wear, corrosion, and heat-resistant dielectric and ornamental coatings⁽¹⁻⁴⁾. In recent years, titanium and Ti-based alloys are widely used in the field of biomedical materials, such as dental restorations, orthopaedic prosthetics, dental implant and heart valves⁽⁵⁻⁸⁾ because of their good biocompatibility and good corrosion resistance properties deriving from the formation of oxide films on surface of metals.

It is unimpeachable that the degradation of Ti and its alloys will occur by electrochemical reactions at the interface between surface of titanium alloys and saliva, inducing in the breakdown of protective titanium oxide passive films, the release of titanium ion and the decrease of the service life of titanium alloys. In recent years, many ways based on a surface modification to improving the biocompatibility of Ti-based implants have been suggested⁽⁹⁾. MAO's use favours the adaptation of surface composition, crystallographic structure, and morphology to achieve large features that parent metal cannot provide. The MAO process mechanism is based on the anodizing electrochemical reaction that happens on a metallic surface and is followed by micro-arc discharge to create an oxide ceramic surface layer with specific morphology and phase composition^(10,11). Also, coating metals with polymer films is a useful strategy that is of great interest for modification of Ti and its alloys in dental applications since it can modify the properties of the

metal surface and/or protect it from corrosion. Electrochemical polymerization is the best technique for manufacturing thin films on metal surfaces in order to protect them from corrosion since it enables the synthesis of polymeric films directly onto the metal surface starting from solutions of the relevant monomers (12-14).

The significant element of clove oil is eugenol (4-allyl-2-methoxyphenol), a methoxyphenol with a brief hydrocarbon chain⁽¹⁵⁾. Eugenol has been used as a spice because of its strong odour and as a dental antiseptic. It has been widely used for sedation in patients with toothache, pulpitis, and dental hyperalgesia as a therapeutic agent in dentistry⁽¹⁶⁾. Pharmacologic studies have demonstrated that eugenol has local anaesthetic⁽¹⁷⁾, bacteriostatic and bactericidal,⁽¹⁸⁾ anticandidal,⁽¹⁹⁾ and antifungal⁽²⁰⁾ properties.

In this work, the ceramic coating is formed on pure titanium (Gr.2) and Ti-6Al-4V alloys (Gr.5) in alkaline electrolyte then forms a thin film of poly eugenol (PE) on modification Ti and alloys surface by electro-polymerized of eugenol. The electrosynthesis of polyeugenol (PE) coatings were characterized by FTIR, X-ray and scanning electron microscopy (SEM), coating adhesive where measured in order to assess their surface morphologies. The biological activity for PE coating against several bacteria and oral fungi were studied also.

2. MATERIALS AND METHODS:

2.1. Titanium Preparation:

Titanium specimens of 2 × 2 cm² area were obtained from commercially pure titanium sheet (Gr.2) of 0.5mm thickness, while circular shape samples of Ti-6Al-4V alloys (Gr.5) were mechanically cut with dimensions of 1cm diameter and 4-5 mm thickness. These samples were polishes with emery papers in different grade include 600, 800, 1200 and 2000 mesh grit, and then washed with tap water, distilled water then ethanol and finally with acetone then dried by using a hair drier. Before electrochemical polymerization, titanium specimens were treatment by heating (500°C) to form a barer titanium oxide thin film which increase the current between electrode and eugenol solution.

2.2. Artificial Saliva Preparation:

Reference electrolyte was used named; modified Fusayama artificial saliva which prepared according to a method that has been described in a previous detail report⁽²¹⁾, which closely resembles natural saliva, with composition of (0.4g/l KCl, 0.4g/l NaCl, 0.906g/l CaCl₂.2H₂O, 0.69g/l NaH₂PO₄.2H₂O, 0.005g/l Na₂S.9H₂O and 1g/l urea)., and pH of this electrolyte was 6.2.

2.3. Micro Arc Oxidation of Ti and Ti alloys:

For MAO an AC power of 150 V was employed for (180 sec.). A titanium plate was used as an anode with a large titanium sheet as the cathode electrode in electrolyte contained 10g/L KH₂PO₄ and 0.5g/L KOH, The electrolyte temperature was kept constant at 25°C. After the MAO process, the samples were washed with distilled water and dried at room temperature. Figure (1) shows MAO cell.

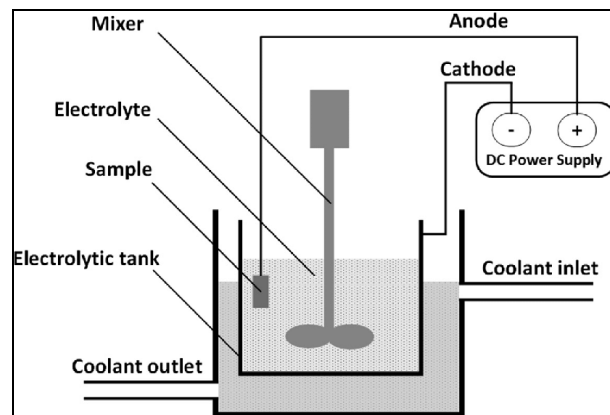


Figure 1. Micro Arc Oxidation cell.⁽²²⁾

2.4. Electrochemical Polymerization of Eugenol:

After heating titanium electrode, it was placed in 0.1M NaOH containing 10mM eugenol and it is necessary to use a large sheet of titanium as counter electrode, the voltage of (3 V) was applied at room temperature with duration (90 min.), then the electrode washed by distilled water and dry by hair drier.

2.5. Characterization and test:

Spectroscopic analysis of eugenol and polyeugenol coated formed with Fourier transform infrared spectroscopy. The surface morphologies of PE coating were measured and analyzed by XRD and SEM. The galvanostatic polarization was measured using WENKING M Lab. (Germany) device. Polarization curves were achieved for dental titanium alloys before and after MAO treatment. TGA of the obtained coated polymers was performed using a Shimadzu DT-30 thermal analyzer (Shimadzu, Kyoto, Japan). And the weight loss for the polymeric coating (PE) was measured at temperature ranging from 25 up to 600°C, at the rate of 10°C/min to determine the degradation rate of the polymer film. The PE coating was tested for antimicrobial activity by well diffusion method against pathogenic bacteria such as *Gram-negative [Escherichiacoli (E-coli), Acinetobacter baumannii (A-baumannii)]* and *Gram-Positive [Staphylococcus aureus (S-aureus), and Bacillus subtilis (B-subtilis)]*. and coating was tested for antimicrobial activity by well diffusion method against and oral fungi such as *Candida albicans (C-Albicans), Candida glabrata (C-glabrata)*,

Candida parapsilosis (*C-parapsilosis*) and *Candida tropicalis* (*C-tropicalis*).

3. RESULT AND DISCUSSION:

3.1. Chemical Structure and Morphology of the Polymeric Eugenol:

Monomeric eugenol exists in the form of a corresponding phenolate anion under conditions applied in this work (0.1 M NaOH). It is well documented that phenolate ions undergo electrochemical oxidation to phenolate radicals through one-electron oxidation⁽²³⁾. These radicals are known to be produced from unsubstituted phenol, resulting primarily in para-coupling, resulting in linear polyphenylene oxide⁽²⁴⁾. On the other hand, two-electron oxidation accompanied by the loss of the methoxy-substituent would produce 4-allyl-1,2-quinone⁽²⁵⁾. As known from the literature 1,2-quinones are extremely unstable species and undergo a variety of intermolecular reactions leading to an ill-defined highly cross-linked polymeric structure⁽²⁵⁾.

Probably, the allyl group is also involved in the polymerization since it is expected to be susceptible to the attack of free radicals and to take part in so-called Diels-Alder reactions between 1,2-quinone (diene) and the allyl C=C bond (dienophile)⁽²⁶⁾. Finally it should be mentioned that at sufficiently high electroodic potential an oxidative degradation of the polymer may occur which will result in the creation of additional oxygen-containing functionalities most likely carbonylic and carboxylic ones or in an extreme case in the generation of carbon dioxide whose presence in the polymeric structure is clearly seen by infrared spectroscopy as discussed below.

To get more information about the structure of the PE formed on titanium plate and to identify functional groups present in it, reflectance FT-IR spectra were recorded for the monomer and polymer formed on a titanium plate by electrochemical polymerization, which is shown in Figure (2).

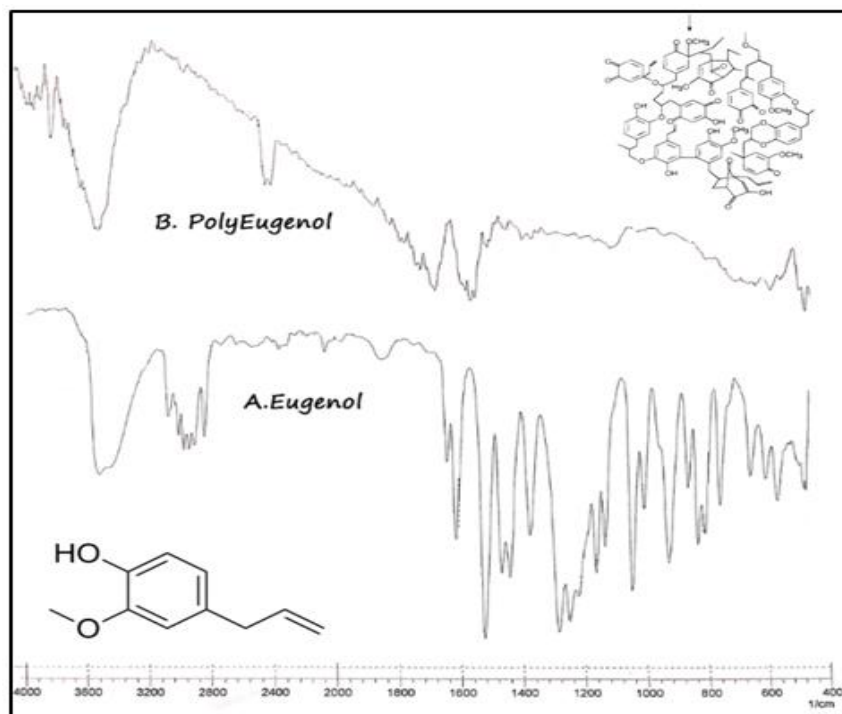


Figure 2. FTIR spectra of a) Eugenol, b) Hypothesized PolyEugenol.

Bands at 3465 and 3436 cm^{-1} , respectively, are assigned to the hydroxyl stretch groups in phenol, and the band at 1539 cm^{-1} possibly indicate for C=O stretch of sodium carboxylate salts of the polymer in alkaline solution. The band at 1639 cm^{-1} may be assigned to the C=O stretch of carbonate groups included in the polymeric film on titanium plate.

Examination of the electropolymerized PE films on Gr.2 and Gr.5 surfaces before MAO treatment using

scanning electron microscopy (SEM) is shown in Figure (3). As seen in the photograph the PE thin film was accumulation on titanium surface before MAO. After magnification to 10K and 100K X shaped structure of PE is evenly distributed hexagonal Nano-structures that tend to aggregate in characteristic cluster forms with intervening porosity. The average partials size of PE deposited on Gr.2 and Gr.5 about (32nm) and (49nm) respectively. Figure (3e and f) show the cross-section SEM for the thin film of PE and enable measurements of

the thickness of poly thin-film to reach to (445nm) and (282nm) for Gr.2 and Gr.5 respectively.

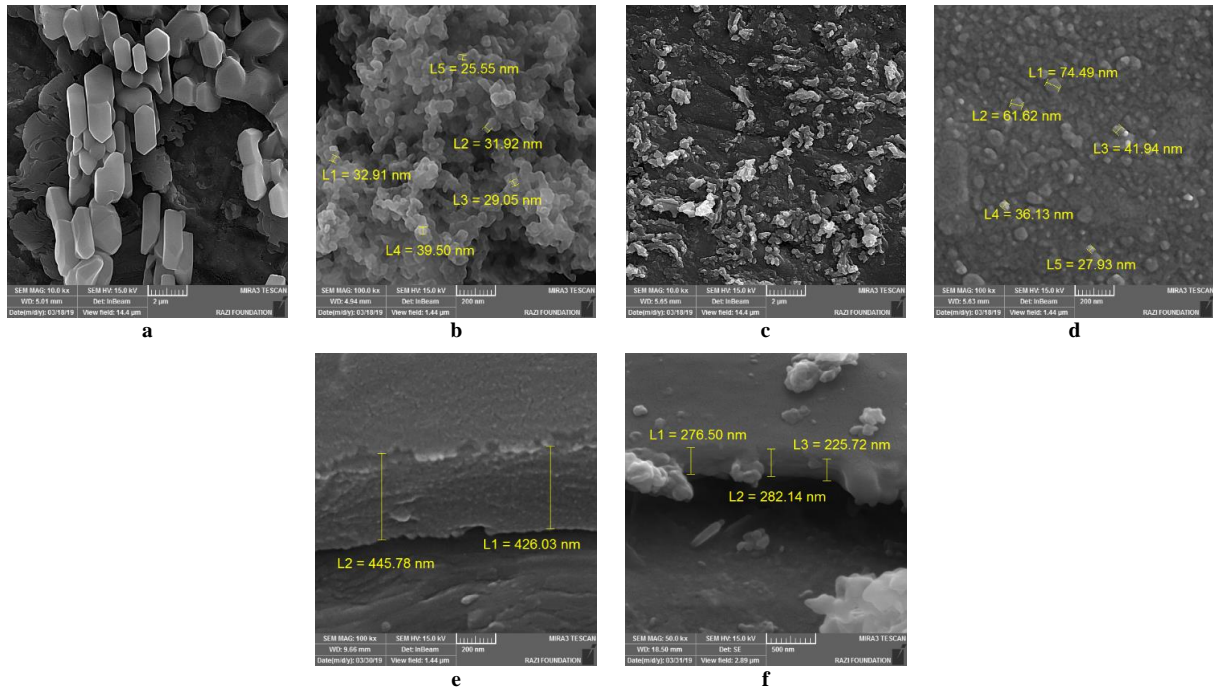


Figure 3. Scanning electron micrographs of PE films deposited on (a and b) Gr.2 (c and d) Gr. 5 and Cross Section Scanning electron micrographs of PE films deposited on (e) Gr.2 (f) Gr.5.

Figures (4) show Gr.2 and Gr.5 alloys after MAO treatment with and without PE films on their surfaces, Figure (4) shows the deposition of PE on the surface of titanium after 150 V MAO process, from the cross-section (Fig. 6d), the PE deposition in the porous Gr.5 surface. The average partial size of PE deposited on Gr.2 and Gr.5 after MAO treatment around (33nm) and (58nm) respectively.

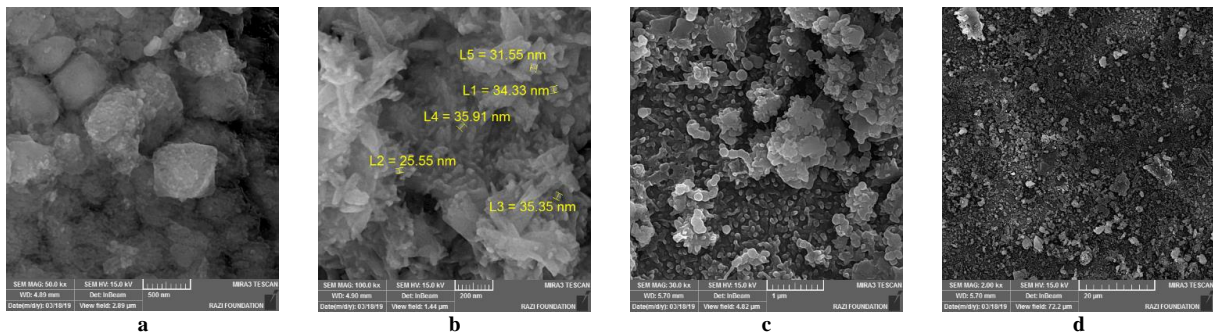


Figure 4. Scanning electron micrographs of PE films deposited on a, b) Gr.2 after MAO treatment, d) Gr.5 after MAO treatment.

The X-ray diffraction features of the blank Gr.2 and for PE formed on Gr.2 by electro-polymerization method are displayed in Figure (5), the XRD pattern for the Gr.2 coated by PE before and after MAO is shown in Figure (5B and 5C), and the peak positions are slightly shifted to lower 2-theta (2θ) values compared to that uncoated Gr.2 and The two high-intensity peaks in Figure (5B) located at 2θ are (25.1° and 25.3°) of polymeric film of eugenol on titanium plate but a small peak in Figure (5C) located at 2θ are (25.38°) may be for PE or formation of titanium oxide layer from MAO process. The crystallite size of the polymeric film was calculated from the full

width at half maximum (FWHM) of the peaks using Debye–Scherrer’s approximation (Eq. 1)

$$d = \frac{k\lambda}{\beta \cos\theta} \dots \dots (1)$$

Where d is the crystallite size, k is the wavelength of CuKα radiation ($k = 1.542\text{Å}$), β is FWHM for the diffraction peak under consideration (in radians), θ is the diffraction angle, and k is the broadening constant ($k=0.9$).

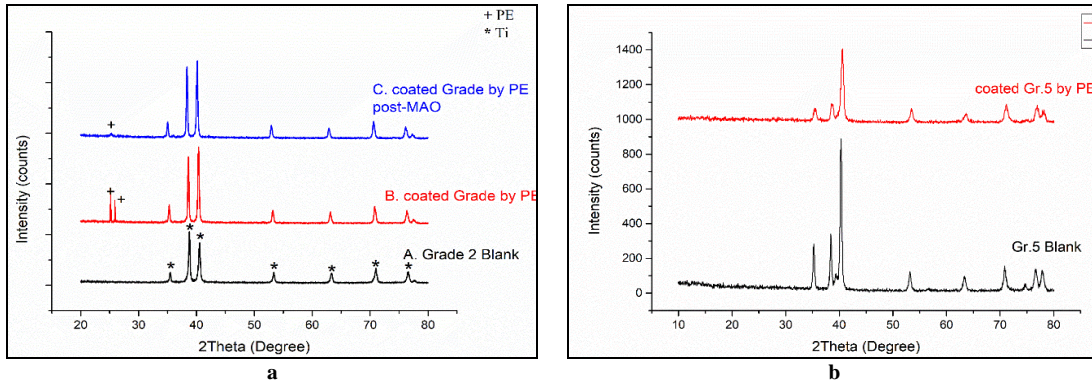


Figure 5. XRD patterns for (a) Gr.2, (b) Gr.5.

The crystallite size has been detected for pure titanium and have the average size equal to (227.5nm), where the crystalline size for PE peak ((25.1° and 25.3°) was equal to (18.99nm) while the size of the average partial of P.E deposited on pure Ti in SEM was about (32 nm).

3.2. Corrosion test:

The Tafel curves for the corrosion test for pure titanium (Gr.2) and for (Gr.5) immersed in artificial saliva before and after electrochemical polymerization by PE at different temperatures were recorded and plotted in Figure (6). The polarization curves of uncoated (Gr.2) show corrosion potential ranged between (-146.7 to -

165.7 mV) and this potential shifted to (-743.2mV) at 293K after coated (Gr.2) by PE, while E_{corr} of uncoated (Gr.5) alloy were ranged between (-556.3 to -485.5mV) then these potentials shifted to more noble potential when Gr.2 surface coated by PE were ranged between (-95 to -149.9mV) Figure (6). E_{corr} for Gr.5 at temperature range (293-323K) have high negative values compared with E_{corr} values for Gr.2, coating Gr.5 led to increase E_{corr} values to noble direction this indicate that Ti alloys are difficult to corrode after coated by PE. It is clear in figure (6b) that E_{corr} for Gr.2 coated by PE were shifter to more noble direction with increasing temperature from 293 to 323 K.

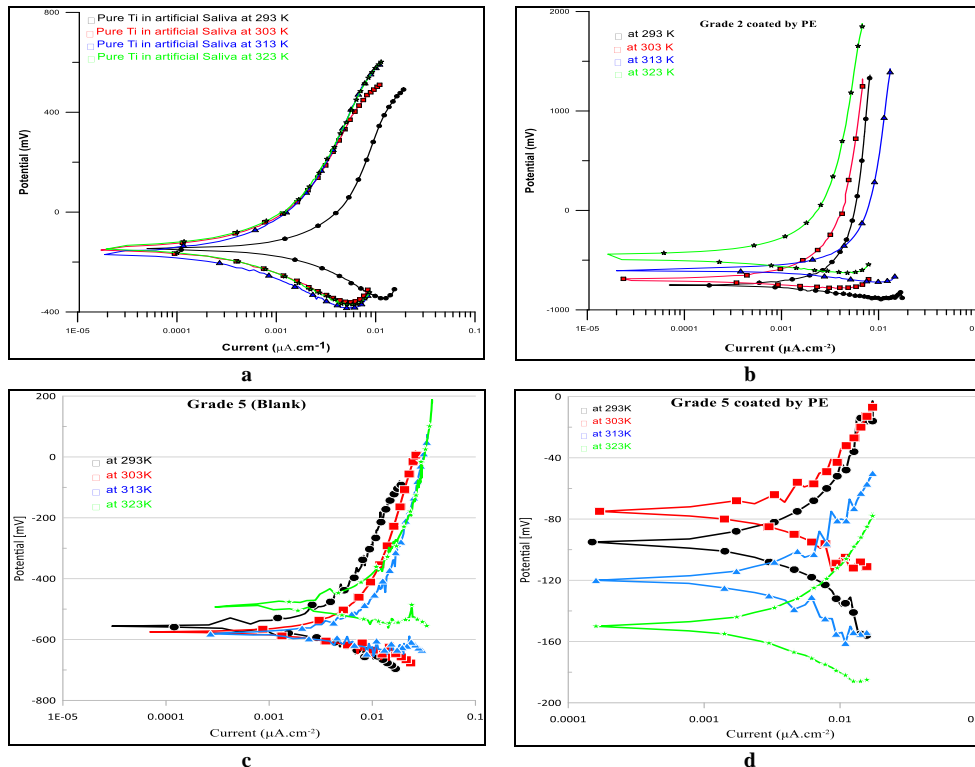


Figure 6. Polarization curves for a) Uncoated Gr.2, b) Gr.2 Coated by PE, c) Uncoated Gr.5 and d) Gr.5 Coated by PE.

Data in the table (1) shows that the corrosion current density, slightly increased with temperature increased for both Gr.2 and Gr.5 but after coated by PE the corrosion current density for Gr.2 have not any effect with increasing temperature, while the i_{corr} for Gr.5 was increased slightly with increased temperature which were ranged between (0.6 to $0.679\mu A.cm^{-2}$), this results indicate that the efficiency of PE against corrosion increased at high temperature.

The Protection Efficiency (%I) can be calculated by using the equation^(26, 27):

$$\%I = \frac{(i_{corr})_b - (i_{corr})_p}{(i_{corr})_b} \times 100 \dots (2)$$

Where $(i_{corr})_b$ and $(i_{corr})_p$ are the corrosion current density ($\mu A.cm^{-2}$) for Blank Gr.2 and Gr.5 and for protected Gr.2 and Gr.5 respectively.

The best %I were obtained after coated Gr.2 by PE which reached to 50% at 293K, while the best %I which were obtained after coated Gr.5 by PE ranged between (70-80)% table (1) data shows that %I slightly increased with increasing temperature, that indicate i_{corr} for Ti coated by PE was not affected by increasing temperature while it lead to increase efficiency of polymer deposit on titanium against corrosion.

E_{corr} values for Gr.2 were higher than E_{corr} values for Gr.5, while E_{corr} values for Gr.5 coated by PE were higher than Gr.2 coated by PE, and the %I obtained by PE coating for Gr.5 higher than %I for PE coating for Gr.2.

Coating by PE led to a protective layer against temperature for the two samples Gr.2 and Gr.5 where the %I increase with temperature increased, and the highest

%I value is 80.37% for coated Gr.5 by PE at 323K. Polarization near the corrosion potential E_{corr} is conducted to determinate the polarization resistance on the basis of the following equation, i.e., the Stern–Geary equation:

$$R_p = \frac{\Delta E}{\Delta i} = \frac{b_a b_c}{2.303(b_a + b_c)} \cdot \frac{1}{i_{corr}} \quad (3)$$

where R_p is the polarization resistance of the system, ΔE is the difference between the polarization potential E and the corrosion potential E_{corr} , Δi is the difference between the measured current density i and the corrosion current density i_{corr} , and b_a and b_c are the anodic and cathodic Tafel coefficients, respectively.

Polarization resistance has such as requirements to be discussed and the measurements of full polarization curves are particularly helpful for identifying corrosion trouble and initiates reconditioned action^(28,29).

Figure (7) depicts the polarization curves for the corrosion of samples after MAO treatment with and without coated by P.E. The fitted values of the corrosion kinetics parameters for all sample are listed in the Table (2).

The data shows the E_{corr} of Gr.2 after MAO treatment ranged between (-388.6 to -294.1mV) while after coated by P.E the E_{corr} shifted to a more noble direction (95 to 17.4 mV). E_{corr} of Gr.5 after MOA treatment ranged between (-388.2 to -343.7mV) also shifted to more noble direction when coated by P.E (109.2 to 186.7mV). Figure (7) show the corrosion potential of Gr.2 shifted to more noble direction with temperature increasing except Gr.2 coated by PE after MAO treatment shifted to more active potential.

Table 1. Corrosion kinetic parameters for Gr.2 and Gr.5 before MAO in artificial saliva at different temperature in the range (293-323)K.

Temp./K		$-E_{corr}/mV$	$I_{corr}/\mu A.cm^{-2}$	$-b_a/mV.dec^{-1}$	$b_c/mV.dec^{-1}$	%I	$R_p/\Omega.cm^2$
Blank of Gr.2	293	-146.7	1.41	226	336.4	-	41629.96
	303	-151.0	1.50	258.1	423.3	-	46413.99
	313	-165.7	1.60	282.8	455.5	-	47350.11
	323	-147.7	1.65	249	574.8	-	45721.07
Gr.2 coated by PE	293	-743.2	0.702	70.3	204.0	50.21	32339.153
	303	-688.4	0.669	80.9	122.8	55.40	31654.52
	313	-598.9	0.667	99.2	188.2	58.31	42288.74
	323	-555.8	0.602	102.7	171.8	63.52	46361.85
Blank of Gr.5	293	-556.3	2.010	144.8	301.5	-	21131.92
	303	-572.8	2.590	149.8	368.4	-	17854.19
	313	-577.8	3.010	205.8	489.3	-	20898.39
	323	-485.5	3.460	241.3	532.8	-	20842.72
Gr.5 coated by PE	293	-95.4	0.600	18.1	17.7	70.14	6476.25
	303	-75.4	0.636	16.3	15.6	75.44	5442.15
	313	-120.2	0.650	15.4	18.0	78.40	5544.21
	323	-149.9	0.679	19.3	18.0	80.37	5956.03

Table (2) show corrosion kinetics parameters for the two titanium samples treated by MAO coated and uncoated by PE. i_{corr} values for Gr.2 after MAO treatment were ranged $(0.692 - 1.08)\mu A.cm^{-2}$ while after coated by PE the i_{corr} reduced to $(0.495 - 0.519)\mu A.cm^{-2}$ at temperature ranged (293-323)K. i_{corr} values for Gr.5 after MAO treatment were higher than Gr.2, ranged $(1.17 -$

$1.93)\mu A.cm^{-2}$ while after coated by PE decreased to $(0.569 - 0.644)\mu A.cm^{-2}$, this reduces i_{corr} which give %I reach to 64% and 71% for Gr.2 and Gr.5 respectively and this value increases with temperature increased reach to 68% and 81% for Gr.3 and Gr.5 respectively, where i_{corr} slightly effected by temperature.

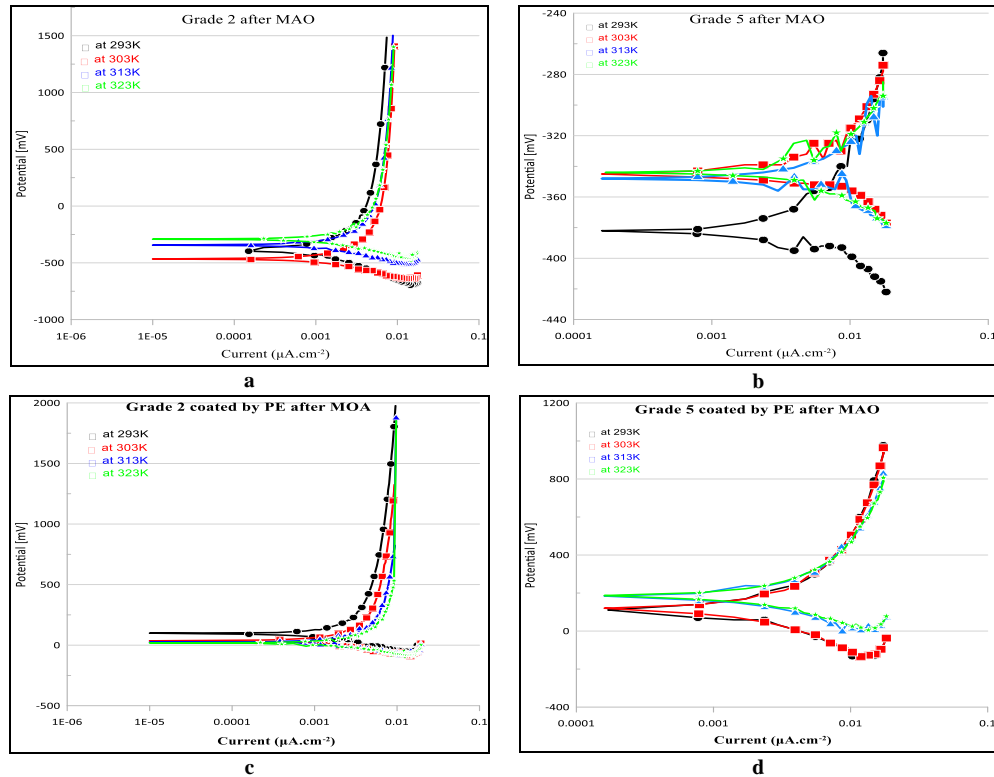


Figure 7. Polarization curves for a)Gr.2 after MAO, b) Gr.2 Coated by PE after MAO, c)Gr.5 after MAO and d) Gr.5 coated by PE after MAO.

Table 2. Corrosion kinetic parameters for Gr.2 and Gr.5 after MAO treatment in artificial saliva at different temperature in the range (293-323)K.

Temp./K	E_{corr}/mV	$I_{corr}/\mu A.cm^{-2}$	$-ba/mV.dec^{-1}$	$bc/mV.dec^{-1}$	%I	$R_p/\Omega.cm^2$	
Gr.2 after MAO	293	-388.6	0.692	194.9	335.8	50.92	77382.61
	303	-471.0	0.841	136.7	249.8	43.93	45616.45
	313	-344.0	0.914	147.8	239.5	42.87	43420.25
	323	-294.1	1.080	152.9	294.0	34.54	40441.45
Gr.2 coated by PE after MAO	293	95.0	0.495	98.9	110.9	64.89	45858.85
	303	35.4	0.504	66.3	99.7	66.40	34306.47
	313	25.2	0.511	61.8	74.9	68.06	28773.11
	323	17.4	0.519	51.3	67.4	68.54	24370.54
Gr.5 after MAO	293	-382.2	1.170	19.2	36.7	41.79	4678.16
	303	-345.3	1.290	9.8	26.4	50.19	2405.68
	313	-347.9	1.710	22.7	21.7	43.18	2817.17
	323	-343.7	1.930	26.2	54.0	44.21	3968.89
Gr.5 coated by PE after MAO	293	109.2	0.569	121.1	153.9	71.69	51718.25
	303	118.7	0.588	133.6	124.6	77.29	47609.87
	313	184.8	0.629	108.7	105.9	79.10	37029.78
	323	186.7	0.644	100.2	99.3	81.38	33627.54

3.3. Kinetic parameters for the corrosion process:

From logarithm of corrosion current density plotted against reciprocals temperature for the corrosion of uncoated, coated Gr.2 and Gr.5 by PE before and after

MAO treatment can obtain the data in the table (3) and shows the activation energy increased after MAO treatment, change from $(4.232 kJ.mol^{-1})$ to $(11.173 kJ.mol^{-1})$ and from $(14.056 kJ.mol^{-1})$ to $(15.833 kJ.mol^{-1})$

for Gr.2 and Gr.5 respectively, while after coated titanium by P.E before and after MAO treatment, the activation energy decreased and Arrhenius factor also

decrease that indicated decrease in the number of corrosion sites on Gr.2 and Gr.5 alloys surface.

Table 3. Kinetic parameters for Gr.2 and Gr.5 in artificial saliva.

	Gr.2		Gr.5	
	Ea/ kJ.mol ⁻¹	A x10 ²⁴ Molecules.cm ⁻² .S ⁻¹	Ea/ kJ.mol ⁻¹	A x10 ²⁶ Molecules.cm ⁻² .S ⁻¹
Blank	4.232	4.84	14.056	3.98
Post MAO	11.173	41.3	15.833	3.21
Coated by PE	3.622	0.096	2.792	0.016
Coated by PE post-MAO	1.277	0.493	2.792	0.016

3.4. The Thermodynamic Studies:

The change in the entropy (ΔS^*) for transition state of corrosion process could be derived according to modified Arrhenius equation:

$$\log \frac{i_{corr}}{T} = \log \frac{R}{Nh} + \frac{\Delta S^*}{2.303R} - \frac{\Delta H^*}{2.303RT} \quad (4)$$

Where i_{corr} is the corrosion current density of titanium in artificial saliva derived from Tafel plot, h is the Plank's constant, N is the Avogadro number, ΔS^* is the activation entropy and ΔH^* is activation enthalpy. The plot of $\log i_{corr}/T$ against $1/T$ obtained straight lines with the slope and an intercept.

Values of ΔS^* which presented in the table (4) reflect the changes in the order and transition state orientation of corrosion process of Gr.2 and Gr.5, and the data in the Table (4) shows the values of ΔS^* were slightly effected by protected coating. Enthalpy of activation ΔH^* is a

component of activation energy, for this note the values of ΔH^* linked to the values of (E_a). The coated Gr.2 by PE before and after MAO treatment has ΔH^* changed from endothermic to exothermic, while coated Gr.5 by PE before and after MAO led to decrease the value of activation enthalpy, but the treatment of Gr.2 and Gr.5 by MAO cause an increase in ΔH^* values.

The free energy change of electrochemical corrosion reaction transition state can be calculated using the following equation:

$$\Delta G^* = \Delta H^* - T\Delta S^* \quad (5)$$

The values of ΔG^* took positive values and showed almost small change with increasing temperature, indicating that the activated complex was not stable and the probability of its formation decreased somewhat with rising in temperature⁽³⁰⁾

Table 4. Kinetic and thermodynamic parameters for Gr.2 and Gr.5 in artificial saliva at temperature range (293-323)K.

		$\Delta G^*/\text{kJ.mol}^{-1}$				$\Delta H^*/\text{kJ.mol}^{-1}$	$\Delta S^*/\text{kJ.mol}^{-1}.\text{K}^{-1}$
		293	303	313	323		
Gr.2	Blank	70.87	73.23	75.59	77.96	1.675	-0.236
	Post MAO	72.59	74.77	76.95	79.14	8.616	-0.218
	Coated by P.E	72.56	75.25	77.94	80.63	-6.178	-0.268
	Coated by P.E post-MAO	73.43	75.98	78.53	81.09	-1.329	-0.255
Gr.5	Blank	69.96	71.95	73.95	75.94	11.499	-0.199
	Post MAO	71.41	73.46	75.50	77.55	11.456	-0.205
	Coated by P.E	73.22	75.70	78.18	80.66	0.541	-0.248
	Coated by P.E post-MAO	72.91	75.39	77.87	80.35	0.236	-0.248

3.5. TG/DSC analysis:

TG /DSC curves for PE thin film formed on titanium show weight loss at four regions as shown in Figure (8). The first one occurs in the region between 20 and 75°C which is assigned to the loss of weight of about 5% due to absorbed water. The second stage recorded a mass change of 10% at 186°C, and is the loss of water of lattice accompanied by a small endothermic at peak 299 °C. The gradual loss of mass from 300 to 600°C is due to the liberation of nitrates and carbonates from precursors. The total mass loss is approximately 42%.

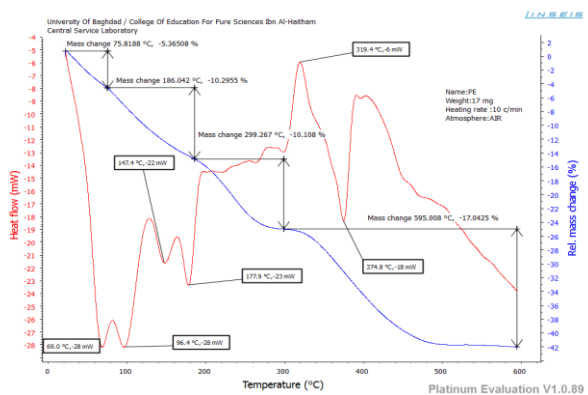


Figure 8. TG/DSC curves for poly eugenol coated on Ti.

3.6. Adhesion Test:

Excellent adhesion of a polymeric coated film on the Ti surface led to good corrosion protection of Ti and Ti alloy. Adhesion testing determines how well a coating is bonded to the Ti surface. The adhesion pull-off testing was performed for different coating types on commercially pure titanium (Gr.2) only because the test is carried out on samples with of dimensions 4 x 4 cm. The values for the failure strength and the type of failure indicate that the PE coating after MAO treatment reach to (1.98 MPa) has stronger adhesive properties than P.E coating on Ti surface before MAO treatment (1.23 MPa) by approximately 0.75 MPa.

3.7. Antimicrobial Activity:

With the expanding rate of microbial species in the oral cavity becoming resistant to present antibiotics, many

studies have attempted and effective antimicrobial reagents of resistance and with low cost. Such problems have led to the resurgence in the use of metal-based antiseptics which are applicable to broader spectrum of bacteria with far lower susceptibility to induce resistance than common antibiotics. The positive control amoxicillin was highly effective against positive gram bacteria and lower effective against negative gram bacteria at 1 mg/mL concentration of and the negative control DMSO does not have any activity against both gram-positive and negative bacteria. The highest antibacterial activity was observed against *B.subtilis* for PE coating followed against *B.subtilis* and PE coating against *S.aureus*. The antibacterial activity of PE coating against *E.Coli* was higher than activity of positive control, as shown in table (5).

Table 5. Antibacterial activity (zone of inhibition, mm) of the PE coating.

Bacteria	E. Coli	A. baumannii	B. subtilis	S. aureus
Amoxicillin (+ve)	13	14	31	25
PolyEugenol	19	13	25	28
Fungi	C. albicans	C. tropicalis	C. glabrata	C. parapsilosis
Fluconazole (+ve)	28	22	22	22
PolyEugenol	29	20	24	20

The positive control Fluconazole was highly effective against *Candida* species at the concentration of 1 mg/ml. The antifungal activity of coating was tested against four *Candida* species (*C.albicans*, *C.tropicalis*, *C.glabrata* and *C.parapsilosis*) by well diffusion method. The highest zone of inhibition was observed in PE coating against *C.albicans*, as shown in table (5).

CONCLUSION:

Electro-polymerization of eugenol on Gr.2 and Gr.5 surfaces and treatment the surfaces of Gr.2 and Gr.5 by MAO technique were employed to increase the corrosion resistance of these alloys in artificial saliva. From the obtained results, the following conclusions are obtained:

1. The particles size of PE on Gr.2 before and after MAO was around (33nm), not affected by MAO process, while the particles size of PE on Gr.5 increase from (49nm) to (58nm) after treated by MAO.
2. Coating Gr.5 by PE led to shifted the corrosion potential to more noble potential, while Gr.2 coated by PE shifted to more active potential and this coating led to reduce the corrosion current density to 50% and 70% at 293K for Gr.2 and Gr.5 respectively, and it have not any effect with increasing temperature. The protection efficiency of PE against corrosion reaches to 63% and 80% at 323K respectively.
3. Coating Gr.2 by PE after MAO treatment led to increase the protection efficiency to 65% at 293K

and reach to 69% at 323K, while Gr.5 coated by P.E after MAO have not largely effect on %I.

4. The activation energies for the corrosion of treated alloys by MAO were increased, but coated alloys by P.E pre and post-MAO led to decrease A and E_a values, the decreased of A values to decrease in corrosion active sites number on the surface of alloys coated by PE.
5. The adhesion strength of PE film on Gr.2 increased when coated on a treated surface by MAO.
6. The antibacterial activity of PE coating was highest against positive gram bacteria (*S. aureus* and *B.subtilis*) than a negative gram (*E.Coli* and *A. baumannii*).
7. The antifungal activity of PE coating shows good activity against oral fungi (*candida* species).

REFERENCES:

1. Santos-Coquillat A, Tenorio RG, Mohedano M, et al. Tailoring of antibacterial and osteogenic properties of Ti6Al4V by plasma electrolytic oxidation. *Applied Surface Science*. 2018; 454:157-72.
2. Fei C, Hai Z, Chen C, et al. Study on the tribological performance of ceramic coatings on titanium alloy surfaces obtained through microarc oxidation. *Progress in Organic Coatings*. 2009; 64(2-3):264-7.
3. Wang Y, Jiang B, Lei T, et al. Dependence of growth features of microarc oxidation coatings of titanium alloy on control modes of alternate pulse. *Materials Letters*. 2004; 58(12-13):1907-11.
4. Yerokhin A, Nie X, Leyland A, et al. Characterisation of oxide films produced by plasma electrolytic oxidation of a Ti-6Al-4V alloy. *Surface and Coatings Technology*. 2000; 130(2-3):195-206.
5. Albayrak Ç, Hacısalıhoğlu İ, Alsaran A. Tribocorrosion behavior of duplex treated pure titanium in simulated body fluid. *Wear*. 2013; 302(1-2):1642-8.

6. Rautray TR, Narayanan R, Kim K-H. Ion implantation of titanium based biomaterials. *Progress in Materials Science*. 2011; 56(8):1137-77.
7. Kumar S, Narayanan TS. Electrochemical characterization of β -Ti alloy in Ringer's solution for implant application. *Journal of alloys and compounds*. 2009; 479(1-2):699-703.
8. De Almeida L, Bastos I, Santos I, et al. Corrosion resistance of aged Ti-Mo-Nb alloys for biomedical applications. *Journal of Alloys and Compounds*. 2014; 615: S666-S9.
9. Liu X, Chu PK, Ding C. Surface modification of titanium, titanium alloys, and related materials for biomedical applications. *Materials Science and Engineering: R: Reports*. 2004; 47(3-4):49-121.
10. Yerokhin AL, Lyubimov VV, Ashitkov RV. Phase formation in ceramic coatings during plasma electrolytic oxidation of aluminium alloys. *Ceramics International*. 1998; 24(1):1-6.
11. Yerokhin A, Nie X, Leyland A, et al. Plasma electrolysis for surface engineering. *Surface and coatings technology*. 1999; 122(2-3):73-93.
12. AlMashhadani HA, editor. *Corrosion Protection of Pure Titanium Implant by Electrochemical Deposition of Hydroxyapatite Post-Anodizing*. IOP Conference Series: Materials Science and Engineering; 2019: IOP Publishing.
13. Mandracci P, Mussano F, Rivolo P, et al. Surface treatments and functional coatings for biocompatibility improvement and bacterial adhesion reduction in dental implantology. *Coatings*. 2016; 6(1):7.
14. De Giglio E, Cometa S, Cioffi N, et al. Analytical investigations of poly (acrylic acid) coatings electrodeposited on titanium-based implants: a versatile approach to biocompatibility enhancement. *Analytical and bioanalytical chemistry*. 2007; 389(7-8):2055-63.
15. Szabadics J, Erdelyi L. Pre-and postsynaptic effects of eugenol and related compounds on *Helix pomatia* L. neurons. *Acta Biologica Hungarica*. 2000; 51(2-4):265-73.
16. Francis LE, Wood DR. *Dental pharmacology and therapeutics*: Saunders; 1961.
17. Brodin P, Røed A. Effects of eugenol on rat phrenic nerve and phrenic nerve-diaphragm preparations. *Archives of Oral Biology*. 1984; 29(8):611-5.
18. Walsh SE, Maillard JY, Russell A, et al. Activity and mechanisms of action of selected biocidal agents on Gram-positive and-negative bacteria. *Journal of applied microbiology*. 2003; 94(2):240-7.
19. Chami N, Bennis S, Chami F, et al. Study of anticandidal activity of carvacrol and eugenol in vitro and in vivo. *Oral microbiology and immunology*. 2005; 20(2):106-11.
20. Lee S-J, Han J-I, Lee G-S, et al. Antifungal effect of eugenol and nerolidol against *Microsporum gypseum* in a guinea pig model. *Biological and Pharmaceutical Bulletin*. 2007; 30(1):184-8.
21. AlMashhadani HAY. Study the Effect of *Punica Granatum* as Oral Antifungal on the Corrosion Inhibition of Dental Amalgam Alloy in Saliva. 2018.
22. Ibrahim MZ, Sarhan AA, Yusuf F, et al. Biomedical materials and techniques to improve the tribological, mechanical and biomedical properties of orthopedic implants—A review article. *Journal of Alloys and Compounds*. 2017; 714:636-67.
23. Kyriacou DK. *Modern electroorganic chemistry*: Springer Verlag; 1994.
24. Bartlett P, Cooper J. A review of the immobilization of enzymes in electropolymerized films. *Journal of Electroanalytical Chemistry*. 1993; 362(1-2):1-12.
25. Ueda C, Tse DC-S, Kuwana T. Stability of catechol modified carbon electrodes for electrocatalysis of dihydronicotinamide adenine dinucleotide and ascorbic acid. *Analytical Chemistry*. 1982; 54(6):850-6.
26. Abbas HA, Alsaade KAS, AlMashhadani HAY, editors. Study the Effect of *Cyperus Rotundus* Extracted as Mouthwash on the Corrosion of Dental Amalgam. IOP Conference Series: Materials Science and Engineering; 2019: IOP Publishing.
27. Shivakumar S, Mohana K. Studies on the inhibitive performance of *Cinnamomum zeylanicum* extracts on the corrosion of mild steel in hydrochloric acid and sulphuric acid media. *Journal of Materials and Environmental Science*. 2013; 4(3, Cop):448-59.
28. Schorr M, Yahalom J. The significance of the energy of activation for the dissolution reaction of metal in acids. *Corrosion Science*. 1972; 12(11):867-8.
29. Al-Saadie KAS, Al-Mashhdani HAY. Corrosion Protection Study for Caron Steel in Seawater by Coating with SiC and ZrO₂ Nanoparticles. *American Journal of Chemistry*. 2015; 5(1):28-39.
30. Mohammed RA. An investigation of electropolymerization and corrosion protection properties of polypyrrole coating on carbon steel and stainless steel. Iraq: University of Baghdad; 2014.